Journal of Hazardous Materials xxx (xxxx) xxx

Contents lists available at ScienceDirect

Journal of Hazardous Materials

journal homepage: www.elsevier.com/locate/jhazmat

Research paper

Increased adverse effects during metabolic transformation of short-chain chlorinated paraffins by cytochrome P450: A theoretical insight into 1-chlorodecane

Mei Wang, Yanpeng Gao, Guiying Li, Taicheng An *

Guangdong Key Laboratory of Environmental Catalysis and Health Risk Control, Guangzhou Key Laboratory of Environmental Catalysis and Pollution Control, School of Environmental Science and Engineering, Institute of Environmental Health and Pollution control, Guangdong University of Technology, Guangzhou 510006, China

ARTICLE INFO

Editor: Dr. S Nan

Keywords:
Short-chain chlorinated paraffins
Human metabolism
Cytochrome P450 enzymes
Metabolic mechanism
Health risk assessment

ABSTRACT

Short-chain chlorinated paraffins (SCCPs), frequently detected in human tissues or organs, can result in threat to human health by disturbing normal metabolism. However, their metabolism mechanisms and fates are largely unclear. Therefore, to better understand the impacts of SCCPs and their metabolites on the human health, the metabolic mechanism and kinetics of SCCPs by cytochrome P450 enzymes (CYPs) were explored using density functional theory employed 1-chlorodecane as a model SCCPs. The results show that 1-chlorodecane could be readily metabolized by CYPs, and the rate constant reaches up 42.3 s^{-1} in human body. Dechlorination of 1-chlorodecane is unlikely to occur and hydroxylation is dominated via H-abstraction pathways, especially from the intermediate C atom of 1-chlorodecane. The toxicity assessments suggest that the two metabolites, 10-chlorodecan-5-ol and 1-chlorodecanol could exhibit higher bioaccumulation, carcinogenicity and more serious damage on cardiovascular system after the metabolism of 1-chlorodecane. To our knowledge, this is the first study from the viewpoint of theoretical analysis to explore the metabolism of typical SCCPs in human body. It may provide deep insight into the metabolic transformation mechanism of SCCPs and cause the concerns about the adverse effects of their metabolites in human body.

1. Introduction

Short-chain chlorinated paraffins (SCCPs) have drawn growing attention recently and are ranked as a new group of persistent organic pollutants (POPs) under the Stockholm Convention (UNEP, 2017). SCCPs are synthetic chlorinated *n*-alkanes with carbon chain length ranging from 10 to 13 and chlorine content of 30–70% (mass weight) (Feo et al., 2009). They are widely used in metal-working fluids, adhesives, paints, sealants, and leather finishing agents in industrial production as well as lubricant and flame retardants in daily necessities (Fiedler, 2010). Although they have been identified with the characteristics of POPs, such as toxicity (Geng et al., 2016, 2019), persistence (Iozza et al., 2008), long-range transport (Ma et al., 2014) and bioaccumulation (Houde et al., 2008; Sun et al., 2020), SCCPs are still escaped from regulation in most countries of the world. According to emission inventory of SCCPs in China in 2010–2014, the total emissions of SCCPs in 2014 reached 3084 tons (Zhang et al., 2017). Given their extensive usage, SCCPs have been ubiquitous and frequently detected in various environmental matrices including atmosphere (Zhuo et al., 2019), house dust (Hilger et al., 2013), soil (Moeckel et al., 2020), water and food (van Mourik et al., 2016). Continuous exposure to SCCPs further result in the occurrence in human tissue. For example, the concentrations of SCCPs were reported up to 370–35,000, 733 and 98.5–3771 ng/g lipid weight in human blood (Li et al., 2017a), breast milk (Xia et al., 2017)and human placenta (Liu et al., 2020), respectively. Thus, serious concern was increasingly raised about their adverse effects to human health recently, due to the continuous exposure to various organisms as well as human beings.

Long-term exposure to SCCPs have been reported to be associated with the potential adverse effects on organismic health, including carcinogenic toxicity and disturbance of immune, reproductive and metabolism systems. For example, the carcinogenicity of SCCPs have been demonstrated by a 2-year oral exposure study in rats and mice (Bucher et al., 1987). Moreover, SCCPs could induce deformities of zebra fish (Liu et al., 2016) and the incidence of a few diseases such as kidney tumors of male rats (Warnasuriya et al., 2010). SCCPs exposure

* Corresponding author.
E-mail address: antc99@gdut.edu.cn (T. An).

https://doi.org/10.1016/j.jhazmat.2020.124391
Received 12 August 2020; Received in revised form 14 October 2020; Accepted 25 October 2020
Available online 28 October 2020

can disturb significant metabolic pathway by altering the intracellular redox status, and disturb glycolysis and amino acid metabolism by affecting human hepatoma HepG2 cells (Geng et al., 2015). More importantly, it was noticed that only 30% of the oral intake of SCCPs can be detected in rats' feces after metabolic transformation (Geng et al., 2016), indicating that most could be accumulated and transformed with the unknown mechanisms in the human body. Although the metabolism was adopted to explore the toxic assessment of SCCPs in human hepatic cells (Ren et al., 2019) and zebrafish embryos (Ren et al., 2018), the metabolic mechanism of SCCPs is still largely unclear. Moreover, previous reference have systematically studied the transformation of SCCPs in the environment matrixes and biota (Ma et al., 2019), and chlorinated alcohols, dechlorination and lower chlorinated products were formed at atmosphere (Liu et al., 2015) and plants (Li et al., 2017b), while the metabolic transformation products of SCCPs is largely unknown. Therefore, the transformation products and metabolic pathways of SCCPs should arouse more attention in *vivo*.

Generally, the metabolic transformation of exogenous compounds including SCCPs in human body is an extremely complicated processes, and involves the action of many enzymes. Cytochrome P450 enzymes (CYPs) serve as one of the most versatile enzymes known and they are abundant in the liver of various mammals such as animals and human beings. They often act as potent oxidation catalysts (Meunier et al., 2004), mainly involving in the metabolic transformation of various xenobiotic chemicals (Guengerich, 2017). For instance, CYPs are reported to induce the metabolic transformation of brominated flame retardants (Wang et al., 2017) and the monooxygenation reaction of methane to produce hydroxylated products. It is noteworthy that several metabolic products could potentially induce endocrine disrupting effects and develop neurotoxicity (Zhang et al., 2018). In particular, high toxic products such as cancerogenic dioxin could be formed during the metabolic transformation of PBDEs (Fu et al., 2016). Noteworthy, experimental studies have found that CYPs gene was upregulated when SCCPs interferes with the thyroid (Gong et al., 2018) and endocrine effects (Zhang et al., 2016), and the expression of CYPs gene is an important process for the metabolic transformation of pollutants. Interesting, high chlorinated alkanes are more dependent on cytochrome P450 for their degradation to CO_2 (Darnerud, 1984), but the metabolic process and transformation mechanism of 1-chlorodecane was not attempted yet. In short, it is of great significance to probe the metabolic kinetics and mechanism of SCCP by CYPs for the subsequent toxicity assessment. The ECOSAR model, lazar program and Advanced Chemistry Development (ACD/Labs Percepta) platform are helpful approach to reveal the toxicity, carcinogenicity, and adverse health effects of pollutants and its transformation products. These theoretical models have successfully predicted multiple exogenous compounds and their transformation products (Gao et al., 2019). For example, human health impact of the rocket fuel 1,1-dimethylhydrazine and its transformation products (Carlsen et al., 2009).

Nevertheless, it is extremely complicated to discuss the metabolic process of SCCPs in the human body, due to tens of millions of SCCPs homologues and ethical requirement for human body, and it is difficult to experimentally study its metabolic transformation process in *vivo*. Accordingly, few studies reported on metabolic mechanism, and kinetics could limit the evaluation of health risks. It is necessary to perform theoretical calculation method to explore the mechanism and kinetics of SCCPs catalyzed by the model of CYPs. Alternatively, studies have shown that quantum chemical computations based on density functional theory (DFT) well explain the metabolic fate and toxicity mechanism of xenobiotics catalyzed by Cpd I (Zhang et al., 2018; Guo et al., 2020; Ma et al., 2020). Moreover, DFT can accurately predict pathways, products and kinetics for the reactions of chemicals. For instance, 4,4′-dibromodiphenyl (Zhou et al., 2011), and atmospheric reaction rate for SCCPs with·OH (Li et al., 2014). Therefore, density functional theory is also performed in theoretical calculations on metabolic mechanism of SCCPs with CYPs. As such, in this work, taken 1-chlorodecane as the simplest model of SCCPs, including H atom with different sites and Cl atom, theoretical calculation was performed to explore metabolic transformation kinetics and mechanism of SCCPs, DFT method was employed to unveil all the possible pathways during the metabolic transformation of SCCPs catalyzed by CYPs in human body. Furthermore, the adverse effects including bioconcentration, carcinogenicity and cardiovascular system of targeted 1-chlorodecane and their metabolic products during metabolic transformation were discussed from the viewpoint of human health.

2. Computational methods

2.1. Model system

The simplified model of active site of CYPs, the complex $Fe^{4+}O^{2-}(C_{20}N_4H_{12})^{-}(SH)^{-}$ was well adopted to simulate the active site of CYPs according to the previous experience (Ji and Schuurmann, 2013; Zhang et al., 2018), and hereinafter referred to Cpd I in this work. Diverse computational studies have verified the feasibility of utilizing the Cpd I model to explore the mechanism of similar substrates such as alkane (via the C–H hydroxylation) (Cho et al., 2016) and carbon tetrachloride via C–Cl breaking (Hackett et al., 2007). Moreover, previous studies have compared the reactions in the protein environment using the combined quantum and molecular mechanics (QM/MM) method with pure quantum mechanics with the model systems, and the results showed the current model can well represents the real CYP enzyme (Schoneboom et al., 2002; Himo, 2017), although the model cannot accurately consider the limitations of the electrostatic and steric effects by the residues surrounding compound I. This model can effectively reproduce high reactivity of CYP enzyme and uncover molecular mechanisms of P450-catalyzed reactions (Ji and Schuurmann, 2013; Guo et al., 2020). Therefore, considering the advantages mentioned-above, the simplified Cpd I model was used in this study to uncover the metabolic transformation of short-chain chlorinated paraffins (SCCPs) by cytochrome P450. Cpd I involve three unpaired electrons and two closely related spin states in the electronic configuration. That is, the high-spin (HS) quartet and low-spin (LS) doublet states were both observed in this specie, which depended on the electron spin direction on the π* orbitals of iron-oxo and on the a_{2u} orbital of the porphyrin ring (Shaik et al., 1998). Both spin states were fully considered to conduct following calculations in this study.

2.2. Mechanism computation

All structural optimization and energy calculations were performed using the Gaussian 09 software package (Frisch et al., 2009; Gao et al., 2019). The geometry optimization of all the reactants, transition states, intermediates and products were implemented by adopting unrestricted density functional UB3LYP method with basis sets of LANL2DZ for the iron atoms and the 6–31 G** basis set for the remaining atoms. It has been shown that the functional method and the basis set could provide the best performance without increasing computational time for the calculations of CYPs-catalyzed reactions, and it was proven to be reliable according to the previous work (Ji et al., 2014). The combination of B3LYP functional and other basis sets have been widely used in the CYPs metabolism investigations, including the phenolic pollutants (Ji et al., 2018; Guo et al., 2020) and triphenyl phosphate (Zhang et al., 2018). The B3LYP functional can reproduce effectively the detailed description of different spin states of iron porphyrin (Liao et al., 2006), yield geometries in good agreement with experimental crystal structures (Strickland and Harvey, 2007), and show qualitatively accurate relative energies versus benchmark calculations for the heme systems (Altun et al., 2014).

To further access the sensitivity of the reaction mechanism toward the different density functionals, based on the optimized geometries, we performed a benchmark test employing some other functionals,

including TPSSh (Staroverov et al., 2003), B3PW91 (Perdew and Wang, 1992), BLYP (Becke, 1988), MPW1PW91 (Adamo and Barone, 1998), and M06L (Zhao and Truhlar, 2006) through single-point calculations in the high spin, and the results are shown in Table S3. By comparing all pathways under the high spin, we found that some difference of existed for absolute energy barriers for each route, and the relative pathway energies, the reaction preferences were similar to other functionals for each route. Importantly, the relative preference of the pathways are thus insensitive to method choice. Furthermore, the study also confirmed that the B3LYP functional performs was the best tested functionals for simulating heme systems (Altun et al., 2014), we therefore adopted the B3LYP functional in this work.

At the meantime, the vibrational frequency was calculated at the same theoretical level to determine the transition state (only one imaginary frequency) and to obtain zero-point energy (ZPE), or the stable species (no imaginary frequency), to obtain the thermodynamic contributions. The minimum energy pathway (MEP) was achieved using the intrinsic reaction coordinate (IRC) theory to confirm that the transition state correctly connected the reactants with the associated products. It is because the kinetics calculations are sensitive to activation energy, more-accurate energies computational level of SDD basis set on iron and 6–311 + + G** (the remaining atoms) was also employed to calculate the single-point energies of these reactions, and the profile of potential energy surface is constructed in Tables S1 and S2. The protein solvation environment of the cytochrome P450 enzyme system was also simulated with a nonpolar chlorobenzene solvent, using the polarizable continuum model (PCM), in which the dielectric constant ($\varepsilon = 5.62$) was selected with close to the structure of the enzyme hydrophobic cavity (Shaik et al., 2005). B3LYP itself does not include dispersion by design (Grimme, 2006), it is standard expected state of the art to include dispersion corrections in DFT now. We optimized all transition state at B3LYP-D3/ LANL2DZ(Fe)/6–31 G** (other atom) level of theory. The calculation results indicated that the dispersion correction affected the energy, while geometric structure gave only minor differences (See Table S4 and S5). Hence, dispersion interactions were considered by performing single-point energy calculations with the UB3LYP-D3/SDD (Fe) /6–311 + + G** level to improve the accuracy of energies. To get closer to the real human body temperature, the calculated temperature is set as 310 K, which is the normal temperature of human body. Therefore, the final reported relative free energies of the CYP oxidation reactions in this work were estimated by combining UB3LYP-D3/SDD (Fe)/6–311 + + G** (other atoms) single-point energies with PCM solvation and dispersion corrections, as well as Gibbs free energy corrections from optimizations at the B3LYP/LANL2DZ(Fe)/6–31 G**(other atoms) level, unless otherwise stated, specifically.

2.3. Kinetics calculation

The metabolic reaction kinetics were determined based on Eyring equation by Eq. 1 (Eyring, 1935; Truhlar et al., 1983). The rate constant (k) is computed using the described activation mechanism of SCCP reacted with P450 enzymes according to the method described early (Ma et al., 2018).

$$k = \frac{k_B T}{h} \frac{1}{c^0} \exp\left(\frac{-\Delta G^{\neq}}{RT}\right) \quad (1)$$

where k_B is the Boltzmann constant, and h is the Planck constants. T is the temperature about 310 K, c^0 is the concentration defining the standard state, $\Delta G^{\neq}$ is the free energy of activation and R is the gas constant. The rate of H-abstraction reaction significantly influenced by the quantum mechanical tunneling according to early reference (Tarchouna et al., 2003), therefore, tunneling-corrected k value was further calculated using the Wigner (W) method:

$$k_w = k\Gamma(T) \text{ with } \Gamma(T) = 1 + \frac{1}{24}\left(\frac{h\nu}{k_B T}\right)^2 \quad (2)$$

where $\Gamma(T)$ is the temperature-dependent transmission coefficient for tunneling effects, and ν represents the imaginary frequency (cm^{-1}) in the transition state calculated at the UB3LYP/ LANL2DZ(Fe)/6–31 G** (other atoms) level.

2.4. Adverse effects calculation

SCCPs have the potential to bioaccumulate in human body, further causing potential adverse effects such as carcinogenicity and cardiovascular disease on human health. Thus, bioaccumulation, the potential carcinogenicity and cardiovascular disease are very important in the risk assessment of 1-chlorodecane. In this work, the bioaccumulation were estimated using the previously reported regression-based method BCFBAF model (ECOSAR, 2014). The carcinogenicities were evaluated using the Lazar program (Lazar, 2006). Total of 1447 chemicals were selected from the Carcinogenic Potency Project as a training set and 4337 chemicals were also selected from the Kazius/Bursi database as test sets to verify reliability of this method. The probability of adverse effects on cardiovascular systems is obtained using the Advanced Chemistry Development (ACD/Labs Percepta) platform (ACD/labs, 2016).

3. Results and discussion

3.1. Metabolic transformation mechanism of SCCP

1-chlorodecane with the shortest carbon chain and the strong toxicity was selected as a typical SCCPs in this study. The structure of contaminant 1-chlorodecane is first optimized in humoral environment, considering the protein environment and real human body temperature. As shown in Fig. 1, 1-chlorodecane in humoral environment exhibits the linear structure, and its lengths of C–Cl and C–H bond are obtained as 1.83 and 1.10 Å, respectively. Moreover, based on the calculation of natural bond orbital (NBO) charges, its Cl atom (−0.129 e) is much more negative than H atoms (0.225–0.229 e). This result indicates that H atoms of 1-chlorodecane are more favorable for nucleophilic reaction than Cl atom in human body. Herein, for the convenience of discussion, the carbon atoms of 1-chlorodecane were numbered consecutively, and the carbon atom adjacent to Cl atom was numbered as C1 (Fig. 1).

For the active center of cytochrome P450 enzymes, due to its special electronic spin direction, all the two spin states of Cpd I were optimized in humoral environment (Fig. 2). The Fe-S bond is obtained as 2.57 and 2.54 Å in low-spin and high-spin states, respectively. But the obtained O–Fe bond (1.63 Å) in low-spin state is slightly shorter than one in high-spin state (1.64 Å). The small difference in bond length makes it difficult

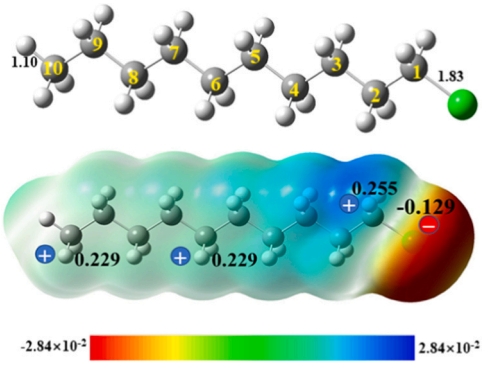

Fig. 1. The optimized and labeled geometries of 1-chlorodecane, as well as the natural bond orbitals analysis (the unit of bond length in Å).

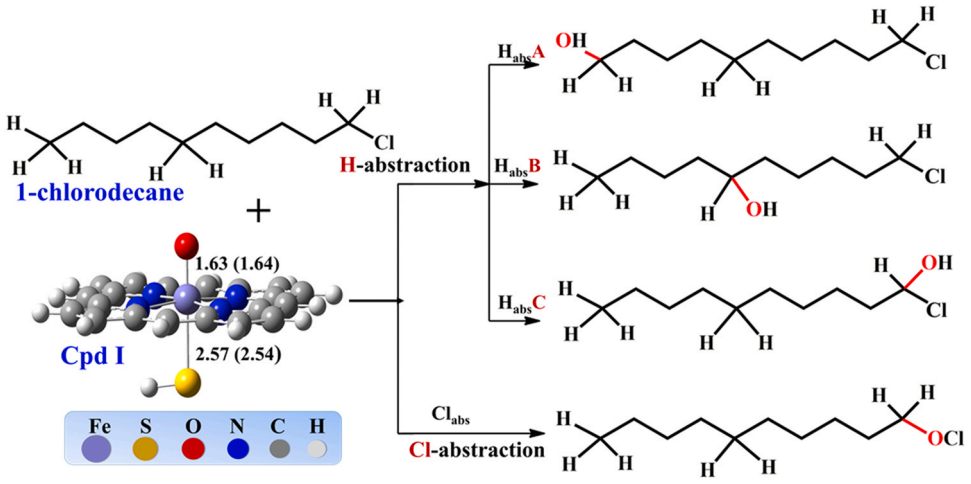

Fig. 2. Schematic diagram of possible reactions of 1-chlorodecane with Cpd I Model structure.

to discriminate the reactivity of O atom in Cpd I at the two-spin state. Thus, the metabolic mechanism of SCCP were fully simulated by P450 enzymes at both the two spin states in humoral environment.

In addition, two different kinds of mechanisms were fully considered in the 1-chlorodecane metabolism by Cpd I: Cl-abstraction (Cl_{abs}) and H-abstraction (H_{abs}) by Fe^{IV}=O of P450 enzyme (Fig. 2). This study focused on H-abstraction routes because the hydroxylation reaction of P450 enzyme is often considered as the metabolism of organic pollutants such as alkanes (Hammerer et al., 2017), aromatic hydrocarbon (Guo et al., 2020) and triphenyl phosphate (Zhang et al., 2018). Previous studies have shown that the dechlorination of perchlorobenzene by P450 can be achieved (Hackett et al., 2007), and H-abstraction and Cl-abstraction can lead to different mechanism by DFT calculation (Ji et al., 2014), the mechanism of Cl-abstraction route on 1-chlorodecane has also been considered. Because of the molecular structure characteristic of 1-chlorodecane, three kinds of possible H-abstraction pathways were illustrated as following: (i) H_{abs}A pathway: H atom abstraction from the terminal methyl group site (C_{10}); (ii) H_{abs}B pathway: H atom abstraction from the middle C atom (C_6); (iii) H_{abs}C pathway, H atom abstraction from the C atom adjacent to Cl atom (C_1). Generally, these transformation pathways occur with different probabilities, although they could occur in parallel. Thus, it is needed to investigate the essence and reactivity of these metabolic pathways from the viewpoint of both thermodynamics and kinetics.

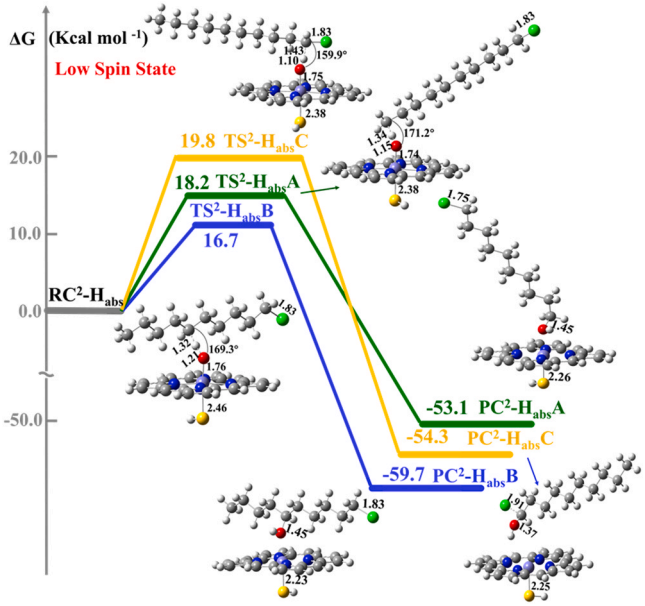

Fig. 3. Free energy profiles for H-abstraction pathways at the low spin state.

3.2. *H-abstraction and Cl-abstraction metabolic pathways*

Firstly, the metabolic transformation of 1-chlorodecane is simulated under the catalysis of enzyme Cpd I at low-spin state. The calculated reaction energy (ΔG) and energy barrier ($\Delta G^{\ddagger}$) of each H-abstraction reaction pathway are shown in Fig. 3. All the H-abstraction pathways (H_{abs}A, B, C) have negative reaction energy values (−53.1 to −59.7 kcal mol^{-1}), meaning that the above metabolic pathways can occur spontaneously in human body. Furthermore, the transition state (TS) of these H-abstraction pathways were observed (Fig. 3), with the imaginary frequencies of *i*798.9, *i*1621.9 and *i*777.3 cm^{-1}, respectively, the imaginary frequencies are similar to those usually observed for H-abstraction processes (Yoshizawa et al., 2001), further ensuring the accuracy of these transition state based on their vibrational mode obtained. Moreover, the structural changes of TS in detailed are discussed in SI. Moreover, the lowest $\Delta G^{\ddagger}$ of 16.7 kcal mol^{-1} was located in pathway H_{abs}B (Fig. 3), which is lower than those of H_{abs}A and H_{abs}C by 3.2 and 1.5 kcal mol^{-1}. The data reveal the H_{abs}B pathway is more favorable than H_{abs}A and H_{abs}C pathways. Noting that C–H bond distance (1.32 Å) in the H_{abs}B transition state was the shortest for the transition states with lower barriers, previous evidence showed that energy difference occurred is mainly due to the difference of geometrical molecular of the transition state between the long C–H bond and the short O–H bond (Yoshizawa et al., 2000). That is, the C–H catalysis by enzyme CYPs at low-spin state could occur more readily at the intermediate C (C6) of 1-chlorodecane in human metabolism, followed by the terminal methyl group (C10) and adjacent to Cl atom (C1) of 1-chlorodecane. Accordingly, the metabolic products, 10-chloro-decan-5-ol, 10-chloro-1-decanol, and 1-chlorodecanol could be formed.

At high-spin state, as shown in Fig. 4, all the H-abstraction pathways also happened spontaneously due to their negative reaction energies (−55.2 to −60.3 kcal mol^{-1}). However, it is noticed that the different stages were observed with the case at low-spin state. It is obvious that the new rebound transition state (TS^4_{red}) existed in metabolism of enzyme Cpd I at the high-spin state (Fig. 4), although the similar structure of initial transition states (TS^4-H_{abs}A, B, and C in Fig. S2) were observed with those at the low-spin state (TS^2-H_{abs}A, B, and C in Fig. 3). As seen from Fig. 4, free energies of the rebound pathway TS^4_{red} are calculated as 6.8, 0.8 and 6.1 kcal mol^{-1} relative to the according reactants (RC^4-H_{abs}). It is noted that the energy barriers of rebound pathways are significantly lower than those of the initial H-abstraction

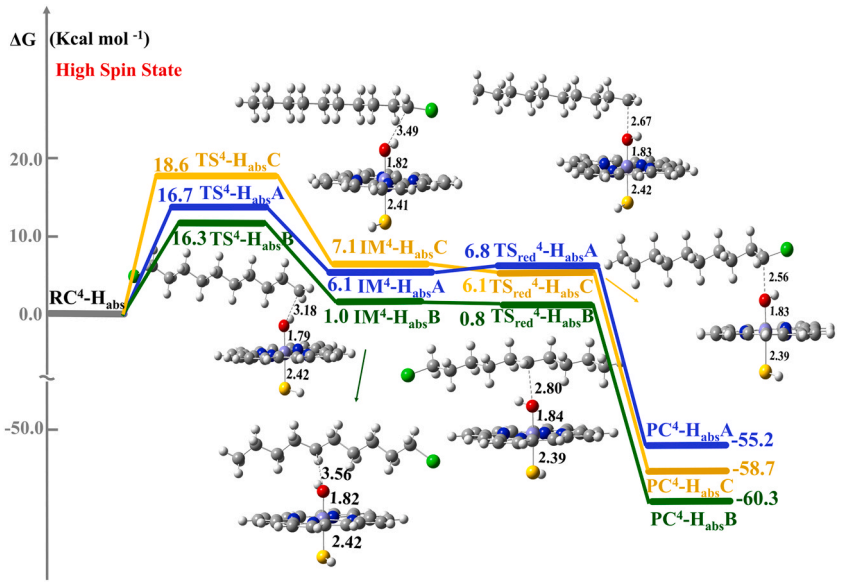

Fig. 4. Free energy profiles for H-abstraction pathways at the high spin state.

(>18.6 kcal mol^{-1}), implying that the H-abstraction step played a very importantly decisive role in the metabolic reaction of 1-chlorodecane. Similar to P450-catalyzed alkane hydroxylation, the HS state produced a significant barrier for rebound, whereas the LS state rebound is essentially barrierless (Shaik et al., 2005, 2008). Moreover, the energy barriers are obtained as 16.7, 16.3 and 18.6 kcal mol^{-1} of pathways H_{abs}A, H_{abs}B and H_{abs}C, respectively. The values were close to the H-abstraction of ethane and propane catalyzed by Cpd I at high-spin (Shaik et al., 2008), and the results show that the pathways H_{abs}A and H_{abs}B could be more conducive pathway. Thus, the main metabolic products, 10-chloro-1-decanol and10-chloro-decan-5-ol, are potentially generated in human body at high spin state.

In short, by comparing three H_{abs} pathways in the metabolic transformation of 1-chlorodecane, H_{abs}A, H_{abs}B and H_{abs}C pathways at high-spin state has lower energy barriers than ones at low-spin state by 1.5, 0.4 and 1.2 kcal mol^{-1}, respectively. The conclusion is different from that the energy barriers of aromatic in the high-spin state were higher than in the low-spin state by 3.0 kcal mol^{-1} (Shaik et al., 2011). The formation of metabolites, chlorinated alcohols, is more prone to occur at the high-spin state than that low-spin state. Compared with previous finding, experiment research has found that CYP52A58 showed an optimal mono-terminal hydroxylation activity toward n-hexadecane for the metabolism of long-chain compounds (Hanano et al., 2015). While the high-spin state of Cpd I may dominates all H_{abs} pathways of metabolic processes, resulting in the metabolites 10-chloro-decan-5-ol, 10-chloro-1-decanol, and 1-chlorodecanol, because a set of P450s of mammalian species cover long-chain fatty acid hydroxylation at various positions (Hlavica and Lehnerer, 2010).

Cl-abstraction pathway could occur in the metabolic transformation of catalyzed by the enzyme Cpd I in humoral environment. Its energy barriers and reaction energy were calculated under the catalysis of enzyme Cpd I at the low and high-spin states, respectively. As seen from Fig. 5, similar to the H-abstraction mechanism, the O–Cl rebound was also observed in high-spin state of enzyme Cpd I reaction. The calculated $\Delta G^{\ddagger}$ of initial step is 47.2 kcal mol^{-1} at the low-spin state, which is only 0.5 kcal mol^{-1} higher than that at high-spin state. Compared with the chlorine extraction energy of chloroform (48.8 kcal mol^{-1}), 1.6 kcal mol^{-1} lower (Ji et al., 2014). The TS^4-Clabs pathway exist a lower barrier of 46.7 kcal mol^{-1}, indicating that the enzyme Cpd I with high-spin state could dominate the reaction of extracting chlorine atoms from 1-chlorodecane. The activation energy for C–Cl breaking displayed high reaction processes, which is consistent with experimental reports

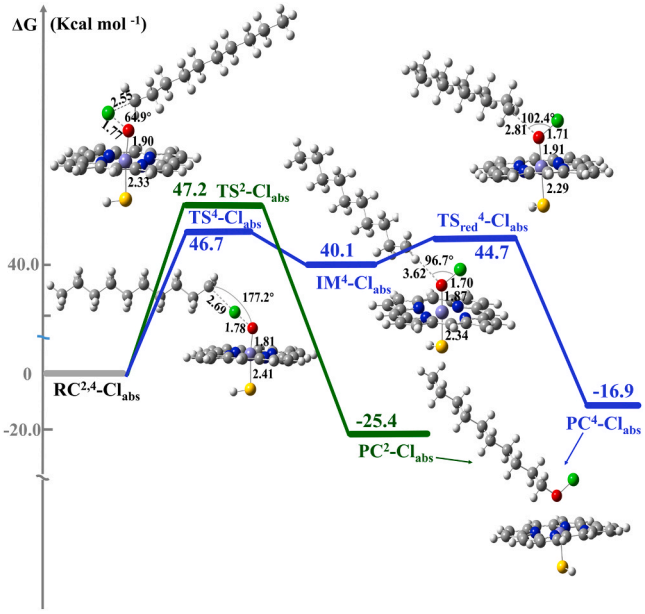

Fig. 5. Free energy profiles for pathway Cl_{abs} at both the low- and high spin states.

on P450 enzymes (Pohl et al., 1984). Moreover, the energy of metabolites PC-Cl_{abs} are obtained as −25.4 and −16.9 kcal mol^{-1} at the low and high spin states, respectively, resulting in the formation of the more stable metabolic products at high-spin state, decyl hypochlorite.

Comparing the two metabolic mechanisms of 1-chlorodecane, the energy barrier of the Cl-abstraction pathway is about at least 26.9 kcal mol^{-1} higher than that of H-abstraction pathways. The data indicate that the Cl-abstraction process could be more difficult to occur in *vivo* than other three H-abstraction pathways, potentially leading to the formation of chlorinated alcohols, 10-chloro-decan-5-ol, 10-chloro-1-decanol and 1-chlorodecanol. Therefore, to distinguish the contribution of each pathway to the metabolic transformation of 1-chlorodecane, further metabolic kinetics calculation is needed to be conducted.

3.3. Metabolic transformation kinetics of SCCP

The metabolic reaction rate constants (k) of each pathway of SCCPs and total metabolic reaction rate constant (k_{total}) are calculated based on above-discussed the metabolic mechanism in *vivo*, as listed in Table S6. The total rate constant of the metabolic transformation of 1-chlorodecane were obtained as 42.3 s^{-1} under the Cpd I degeneracy state. The value of $\Delta G^{\ddagger}$ had a decisive influence on the k. Under the same calculation method, when the $\Delta G^{\ddagger}$ value of H extracted by N′-nitrosonornicotine is 15.4 kcal mol^{-1}, the reaction rate is two orders of magnitude equal 1-chlorodecane, reaching 31.9 s^{-1} (Ma et al., 2018). The k of the four metabolic pathways ($H_{abs}A$, $H_{abs}B$, $H_{abs}C$ and Cl_{abs}) at the low-spin were also calculated as 9.15×10^{-1}, 1.04×10^{1}, 6.81×10^{-2} and 3.27×10^{-21} s^{-1}, respectively. As for the metabolic transformation at the high spin state, $H_{abs}A$ pathway has the same rate as its low-spin state, while $H_{abs}B$, $H_{abs}C$ and Cl_{abs} got rate values of 1.04×10^{1}, 2.00×10^{1}, 4.78×10^{-1} and 7.36×10^{-21} s^{-1}, respectively. Namely, the k at the high-spin state is larger than that at the low-spin state, further indicating that the high-spin pathway could contribute more to the whole metabolic transformation of 1-chlorodecane in human body.

Moreover, it is clear that the k of Cl_{abs} pathway is much smaller than those of three H_{abs} pathways by 22 orders of magnitude (Table S6), explaining that the H_{abs} pathways are dominated mechanism and the Cl_{abs} pathway could be neglected. Moreover, the contribution was expressed by a branching ratios (Γ), which was obtained using the formula $\Gamma = \frac{k}{k_{total}}$, where k and k_{total} represent the rate constant of each pathway and the sum of all pathways. Cl_{abs} pathway is less than 0.01% (Fig. 6). This finding shows that the dechlorination process can be believed not occurred completely in the metabolic transformation of 1-chlorodecane by CYPs. Moreover, the H-abstraction mechanism was similarly dominated in the metabolic transformation of n-hexane by CYPs (Rune Toftgård et al., 1986), but the Cl_{abs} pathway is not always unlikely to occur in the metabolic transformation of organic pollutants, for instance, the metabolism of tetrachloromethane by Cpd I (Ji et al., 2014).

Furthermore, the high-spin pathways could contribute 72.9% to the whole routes. As for the three H-abstraction pathways, the calculated Γs of $H_{abs}B$, $H_{abs}A$ and $H_{abs}C$ are obtained as 71.9%, 26.7% and 1.3%, respectively (Fig. 6). The data imply that the intermediate C atom (C6) of 1-chlorodecane has the highest reaction activity during its metabolic transformation by Cpd I, followed by methyl group C atom (C10) and C atom adjacent to Cl atom (C1). Accordingly, the 10-chloro-decan-5-ol is the dominated metabolites, together with the formation of 10-chloro-1-decanol and 1-chlorodecanol. These metabolic products could be bioaccumulated, and/or continue to metabolize, and thus their certain health risks need to consider their metabolites.

3.4. Bioaccumulation, carcinogenicity and adverse effects on human

The potential adverse effects of the metabolites are necessary to be further investigated due to the high toxicity on human health of original SCCPs. Firstly, the bioaccumulation of 1-chlorodecane and its metabolic products, 10-chloro-decan-5-ol, 10-chloro-1-decanol and 1-chlorodecanol, was calculated using the well-developed models, and the results are shown in Table 1. the logarithm BAF (log BAF) values of the original 1-chlorodecan was 3.2 L/kg wet-wt, and the three metabolites 10-chloro-1-decanol, 1-chlorodecanol and 10-chloro-decan-5-ol with the lower log BAF (2.3 L/kg wet-wt) was obtained. This indicates that 1-chlorodecan are more readily bioaccumulated in the human body, because lipid content was an important factor influencing SCCP bioaccumulation. The log BAF for snakehead, catfish, small mud carp group, and crucian carp group were 2.46, 3.19, 3.25, and 3.45, respectively (Sun et al., 2017), indicating 1-chlorodecan metabolites lower bioaccumulation potential. However, the research showed SCCPs ranged from 1.6 to 3.0 in marine organisms (Huang et al., 2019). Thus, the long-term accumulation of the original 1-chlorodecane and its metabolites could further potentially result in the potential adverse effects on human health, such as cardiovascular system damage and carcinogenicity. Matched well with the adverse health effects caused by SCCPs in previous review, SCCPs and metabolites could pose hepatotoxicity, developmental toxicity, endocrine- and metabolism-disrupting effects, as well as carcinogenicity effects (Wang et al., 2019).

The accumulated 1-chlorodecane and its products may exert toxicological effects in human tissue or organ. Thus, the adverse effects on human cardiovascular system was particularly focused on, due to the potential association between chlorinated paraffins and cardiovascular problems (Zhuo et al., 2019). The probability of the adverse effect on cardiovascular system was elucidated with the ACD/percepta platform. The probability value (P_{cardio}) is between 0 and 1, and the greater the value is, the stronger the adverse effects impose. From Table 1, the P_{cardio} of the metabolites, 10-chloro-1-decanol and 1-chlorodecanol was obtained as 0.34 and 0.33, respectively, nearly three times higher than ones of the original 1-chlorodeance (0.12). These results suggest that the metabolites, 10-chloro-1-decanol and 1-chlorodecanol could causes the more serious adverse effect of on cardiovascular system after the metabolic transformation of 1-chlorodecane.

Furthermore, the carcinogenicity of 1-chlorodecane and its metabolic products were calculated using the recommended method (Tripathi et al., 2018) for the carcinogenicity prediction of nerve medicament. As shown in Tables 1, 1-chlorodecane are found to be carcinogenic, which is agreement with the previous reports (Wang et al., 2018). Moreover, it is noticed that the carcinogenicity of the metabolic products, 10-chloro-decan-5-ol and 1-chlorodecanol still retain, although the one metabolite 10-chloro-1-decanol is non-carcinogenic. Moreover, a previous experimental study have also shown that some SCCPs such as C12 (Cl 60% of SCCPs) may cause carcinogenic effects on the human liver after long-term accumulation, and lead to liver tumor lesions (Bucher et al., 1987). Thus, the carcinogenicity effect of original compound SCCPs as well as their metabolic products is worthy of attention and treatment seriously.

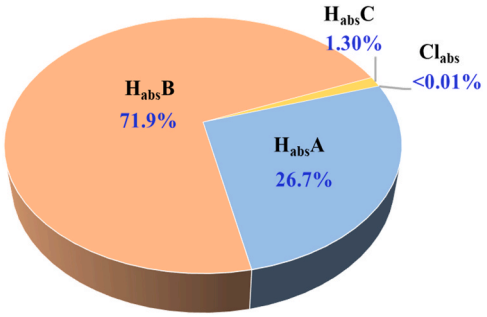

Fig. 6. Branching ratio (Γ) of all reaction pathways.

4. Conclusions

Although the increasing attention on the environmental

Table 1
Bioaccumulation, carcinogenicity and probability of health effect on cardiovascular system effect of 1-chlorodecane and its metabolic products.

Carcinogenicity	1-chlorodecane carcinogen	10-chloro-decan-5-ol carcinogen	10-chloro-1-decanol non-carcinogen	1-chlorodecanol carcinogen
Log BAF (L/Kg wet-wt)	3.2	2.3	2.3	2.3
Cardiovascular system effect	0.12	0.15	0.34	0.33

transformation and health risks of SCCPs (Zhang et al., 2019), the gaps in knowledge still remain regarding their metabolic transformation and metabolites due to the difficult capture in experiment. In particular, the risk assessment considering metabolites is rare. Thus, using theoretical calculation approaches, the metabolic transformation of emerging POPs, SCCPs 1-chlorodecane by cytochrome P450 enzymes (CYPs) was simulated for the first time. 1-Chlorodecane can be readily metabolized by enzyme P450 on both low-spin and high-spin states, although the initial H-abstraction barriers are lower on highs-pin state. We found that 1-chlorodecane was easily transformed at a rate constant of 42.3 s^{-1} by CYPs in human body. The hydroxylation of 1-chlorodecane was more significant than its dechlorination, mainly resulting in three metabolites, 10-chloro-decan-5-ol, 10-chloro-1-decanol and 1-chlorodecanol. Except for the 10-chloro-1-decanol, the carcinogenicity of the other metabolites still remains after the metabolic transformation of 1-chlorodecane. Moreover, because of their high BAF, the bioaccumulated metabolites could potentially causing more serious adverse effect on cardiovascular system under the long-term exposure. Therefore, the health impact of metabolic products together with the original parent SCCPs should be paid more attention in future experimental researches and health risk evaluations.

CRediT authorship contribution statement

Mei Wang: Methodology, Formal analysis, Writing - original draft. **Yanpeng Gao:** Methodology, Data curation. **Guiying Li:** Writing - reviewing & editing. **Taicheng An:** Conceptualization, Supervision.

Declaration of Competing Interest

The authors declare that they have no known competing financial interests or personal relationships that could have appeared to influence the work reported in this paper.

Acknowledgments

This research was financially supported by the National Natural Science Foundation of China (41731279, 41877363 and 41977365), Local Innovative and Research Team Project of Guangdong Pearl River Talents Program (2017BT01Z032), National Key Research and Development Project (2019YFC1804500), The innovation Team project of Guangdong Provincial Department of Education (2017KCXTD012) and Leading Scientific, Technical, and Innovation Talents of Guangdong Special Support Program (2016TX03Z094).

Appendix A. Supporting information

Supplementary data associated with this article can be found in the online version at doi:10.1016/j.jhazmat.2020.124391.

References

Advanced Chemistry Development, 2016. ACD/Labs Percepta, Inc.,Toronto, Ontario, Canada.

Adamo, C., Barone, V., 1998. Exchange functionals with improved long-range behavior and adiabatic connection methods without adjustable parameters: the mPW and mPW1PW models. J. Chem. Phys. 108, 664–675.

Altun, A., Breidung, J., Neese, F., Thiel, W., 2014. Correlated Ab Initio and density functional studies on H_2 activation by FeO^+. J. Chem. Theory Comput. 10, 3807–3820.

Becke, A.D., 1988. Density-functional exchange-energy approximation with correct asymptotic behavior. Phys. Rev. A Gen. Phys. 38, 3098–3100.

Bucher, J.R., Alison, R.H., Montgomery, C.A., Huff, J., Haseman, J.K., Farnell, D., Thompson, R., Prejean, J.D., 1987. Comparative toxicity and carcinogenicity of two chlorinated paraffins in F344/N rats and B6C3F1 mice. Fundam. Appl. Toxicol. 9, 454–468.

Carlsen, L., Kenessov, B.N., Batyrbekova, S.Y., 2009. A QSAR/QSTR study on the human health impact of the rocket fuel 1,1-dimethyl hydrazine and its transformation products multicriteria hazard ranking based on partial order methodologies. Environ. Toxicol. Pharmacol. 27, 415–423.

Cho, K.B., Hirao, H., Shaik, S., Nam, W., 2016. To rebound or dissociate? this is the mechanistic question in C-H hydroxylation by heme and nonheme metal-oxo complexes. Chem. Soc. Rev. 45, 1197–1210.

Darnerud, P.O., 1984. Chlorinated paraffins: effect of some microsomal enzyme inducers and inhibitors on the degradation of 1-^{14}C-chlorododecanes to $^{14}CO_2$ in mice. Acta Pharmacol. Toxicol. 55, 110–115.

ECOSAR, 2014. ⟨http://www.epa.gov/oppt/newchems/tools/21ecosar.htm⟩.

Eyring, H., 1935. The activated complex in chemical reactions. J. Chem. Phys. 3, 107–115.

Feo, M.L., Eljarrat, E., Barceló, D., 2009. Occurrence, fate and analysis of polychlorinated n-alkanes in the environment. Trac Trend Anal. Chem. 28, 778–791.

Fiedler, H., 2010. Short-chain chlorinated paraffins: production, use and international regulations. Chlorinated Paraffins. Springer, Berlin, Heidelberg, pp. 1–40.

Frisch, M.J., Trucks, G.W., Schlegel, H.B., Scuseria, G.E., Robb, M.A., Cheeseman, J.R., Scalmani, G., Barone, V., Mennucci, B., Petersson, G.A., Nakatsuji, H., Caricato, M., Li, X., Hratchian, H.P., Izmaylov, A.F., Bloino, J., Zheng, G., Sonnenberg, J.L., Hada, M., Ehara, M., Toyota, K., Fukuda, R., Hasegawa, J., Ishida, M., Nakajima, T., Honda, Y., Kitao, O., Nakai, H., Vreven, T., Montgomery Jr., J.A., Peralta, J.E., Ogliaro, F., Bearpark, M.J., Heyd, J., Brothers, E.N., Kudin, K.N., Staroverov, V.N., Kobayashi, R., Normand, J., Raghavachari, K., Rendell, A.P., Burant, J.C., Iyengar, S. S., Tomasi, J., Cossi, M., Rega, N., Millam, N.J., Klene, M., Knox, J.E., Cross, J.B., Bakken, V., Adamo, C., Jaramillo, J., Gomperts, R., Stratmann, R.E., Yazyev, O., Austin, A.J., Cammi, R., Pomelli, C., Ochterski, J.W., Martin, R.L., Morokuma, K., Zakrzewski, V.G., Voth, G.A., Salvador, P., Dannenberg, J.J., Dapprich, S., Daniels, A.D., Farkas, Ö., Foresman, J.B., Ortiz, J.V., Cioslowski, J., Fox, D.J., 2009. Gaussian 09. Gaussian, Inc., Wallingford, CT, USA.

Fu, Z., Wang, Y., Chen, J., Wang, Z., Wang, X., 2016. How PBDEs are transformed into dihydroxylated and dioxin metabolites catalyzed by the active center of cytochrome P450s: a DFT study. Environ. Sci. Technol. 50, 8155–8163.

Gao, Y., Li, G., Qin, Y., Ji, Y., Mai, B., An, T., 2019. New theoretical insight into indirect photochemical transformation of fragrance nitro-musks: mechanisms, eco-toxicity and health effects. Environ. Int. 129, 68–75.

Geng, N., Ren, X., Gong, Y., Zhang, H., Wang, F., Xing, L., Cao, R., Xu, J., Gao, Y., Giesy, J.P., Chen, J., 2019. Integration of metabolomics and transcriptomics reveals short-chain chlorinated paraffin-induced hepatotoxicity in male Sprague-Dawley rat. Environ. Int. 133, 105231.

Geng, N., Zhang, H., Xing, L., Gao, Y., Zhang, B., Wang, F., Ren, X., Chen, J., 2016. Toxicokinetics of short-chain chlorinated paraffins in Sprague-Dawley rats following single oral administration. Chemosphere 145, 106–111.

Geng, N., Zhang, H., Zhang, B., Wu, P., Wang, F., Yu, Z., Chen, J., 2015. Effects of short-chain chlorinated paraffins exposure on the viability and metabolism of human hepatoma HepG2 cells. Environ. Sci. Technol. 49, 3076–3083.

Gong, Y., Zhang, H., Geng, N., Xing, L., Fan, J., Luo, Y., Song, X., Ren, X., Wang, F., Chen, J., 2018. Short-chain chlorinated paraffins (SCCPs) induced thyroid disruption by enhancement of hepatic thyroid hormone influx and degradation in male Sprague Dawley rats. Sci. Total. Environ. 625, 657–666.

Grimme, S., 2006. Semiempirical GGA-type density functional constructed with a long-range dispersion correction. J. Comput. Chem. 27, 1787–1799.

Guengerich, F.P., 2017. Intersection of the roles of cytochrome P450 enzymes with xenobiotic and endogenous substrates: relevance to toxicity and drug interactions. Chem. Res. Toxicol. 30, 2–12.

Guo, F., Chai, L., Zhang, S., Yu, H., Liu, W., Kepp, K.P., Ji, L., 2020. Computational biotransformation profile of emerging phenolic pollutants by cytochromes P450: phenol-coupling mechanism. Environ. Sci. Technol. 54, 2902–2912.

Hackett, J.C., Sanan, T.T., Hadad, C.M., 2007. Oxidative dehalogenation of perhalogenated benzenes by cytochrome P450 compound I. Biochemistry 46, 5924–5940.

Hammerer, L., Winkler, C.K., Kroutil, W., 2017. Regioselective biocatalytic hydroxylation of fatty acids by cytochrome P450s. Catal. Lett. 148, 787–812.

Hanano, A., Shaban, M., Almousally, I., Al-Ktaifani, M., 2015. Saccharomyces cerevisiae SHSY detoxifies petroleum n-alkanes by an induced CYP52A58 and an enhanced order in cell surface hydrophobicity. Chemosphere 135, 418–426.

Hilger, B., Fromme, H., Voelkel, W., Coelhan, M., 2013. Occurrence of chlorinated paraffins in house dust samples from Bavaria, Germany. Environ. Pollut. 175, 16–21.

Himo, F., 2017. Recent trends in quantum chemical modeling of enzymatic reactions. J. Am. Chem. Soc. 139, 6780–6786.

Hlavica, P., Lehnerer, M., 2010. Oxidative biotransformation of fatty acids by cytochromes P450: predicted key structural elements orchestrating substrate specificity, regioselectivity and catalytic efficiency. Curr. Drug Metab. 11, 85–104.

Houde, M., Muir, D.C.G., Tomy, G.T., Whittle, D.M., Teixeira, C., Moore, S., 2008. Bioaccumulation and trophic magnification of short- and medium-chain chlorinated paraffins in food webs from Lake Ontario and Lake Michigan. Environ. Sci. Technol. 42, 3893–3899.

Huang, Y., Chen, L., Jiang, G., He, Q., Ren, L., Gao, B., Cai, L., 2019. Bioaccumulation and biomagnification of short-chain chlorinated paraffins in marine organisms from the Pearl River Estuary, South China. Sci. Total. Environ. 671, 262–269.

Iozza, S., Muller, C.E., Schmid, P., Bogdal, C., Oehme, M., 2008. Historical profiles of chlorinated paraffins and polychlorinated biphenyls in a dated sediment core from Lake Thun (Switzerland). Environ. Sci. Technol. 42, 1045–1050.

Ji, L., Ji, S., Wang, C., Kepp, K.P., 2018. Molecular mechanism of alternative P450-catalyzed metabolism of environmental phenolic endocrine-disrupting chemicals. Environ. Sci. Technol. 52, 4422–4431.

Ji, L., Schuurmann, G., 2013. Model and mechanism: N-hydroxylation of primary aromatic amines by cytochrome P450. Angew. Chem. Int. Ed. 52, 744–748.

Ji, L., Zhang, J., Liu, W., de Visser, S.P., 2014. Metabolism of halogenated alkanes by cytochrome P450 enzymes. Aerobic oxidation versus anaerobic reduction. Chem. Asian J. 9, 1175–1182.

Lazar, 2006. Lazar toxicity predictions. ⟨https://lazar.in-silico.ch/predict⟩.

Li, C., Xie, H.B., Chen, J., Yang, X., Zhang, Y., Qiao, X., 2014. Predicting gaseous reaction rates of short chain chlorinated paraffins with ·OH: overcoming the difficulty in experimental determination. Environ. Sci. Technol. 48, 13808–13816.

Li, T., Wan, Y., Gao, S., Wang, B., Hu, J., 2017a. High-throughput determination and characterization of short-, medium-, and long-chain chlorinated paraffins in human blood. Environ. Sci. Technol. 51, 3346–3354.

Li, Y.L., Hou, X.W., Yu, M., Zhou, Q.F., Liu, J.Y., Schnoor, J.L., Jiang, G.B., 2017b. Dechlorination and chlorine rearrangement of 1,2,5,5,6,9,10-heptachlorodecane mediated by the whole pumpkin seedlings. Environ. Pollut. 224, 524–531.

Liao, M.S., Watts, J.D., Huang, M.J., 2006. Assessment of the performance of density-functional methods for calculations on iron porphyrins and related compounds. J. Comput. Chem. 27, 1577–1592.

Liu, L.H., Li, Y.F., Coelhan, M., Chan, H.M., Ma, W.L., Liu, L.Y., 2016. Relative developmental toxicity of short-chain chlorinated paraffins in Zebrafish (*Danio rerio*) embryos. Environ. Pollut. 219, 1122–1130.

Liu, R.R., Zhang, C.X., Kang, L.Y., Sun, X.M., Zhao, Y., 2015. The OH-initiated chemical transformation of 1,2,4,6,8,10,11-heptachloroundecane in the atmosphere. RSC Adv. 5, 37988–37994.

Liu, Y.X., Aamir, M., Li, M.Y., Liu, K., Hu, Y.H., Liu, N., Xu, Y.F., Du, J.Y., Xu, J.R., Liu, W.P., 2020. Prenatal and postnatal exposure risk assessment of chlorinated paraffins in mothers and neonates: occurrence, congener profile, and transfer behavior. J. Hazard. Mater. 395, 122660.

Ma, G., Yu, H., Xu, X., Geng, L., Wei, X., Wen, J., Wang, Z., 2020. Molecular basis for metabolic regioselectivity and mechanism of cytochrome P450s toward carcinogenic 4-(methylnitrosamino)-(3-pyridyl)-1-butanone. Chem. Res. Toxicol. 33, 436–447.

Ma, G.C., Yu, H.Y., Xu, T., Wei, X.X., Chen, J.R., Lin, H.J., Schuurmann, G., 2018. Computational Insight into the activation mechanism of carcinogenic N′-nitrosonornicotine (NNN) catalyzed by cytochrome P450. Environ. Sci. Technol. 52, 11838–11847.

Ma, S., Yu, Y., Yang, Y., Li, G., An, T., 2019. A new advance in the potential exposure to "old" and "new" halogenated flame retardants in the atmospheric environments and biota: from occurrence to transformation products and metabolites. Crit. Rev. Environ. Sci. Technol. 50, 1–49.

Ma, X.D., Zhang, H.J., Zhou, H.Q., Na, G.S., Wang, Z., Chen, C., Chen, J.W., Chen, J.P., 2014. Occurrence and gas/particle partitioning of short- and medium-chain chlorinated paraffins in the atmosphere of Fildes Peninsula of Antarctica. Atmos. Environ. 90, 10–15.

Meunier, B., de Visser, S.P., Shaik, S., 2004. Mechanism of oxidation reactions catalyzed by cytochrome P450 enzymes. Chem. Rev. 104, 3947–3980.

Moeckel, C., Breivik, K., Nost, T.H., Sankoh, A., Jones, K.C., Sweetman, A.. Soil pollution at a major West African E-waste recycling site: contamination pathways and implications for potential mitigation strategies. Environ. Int. 137, 105563.

Perdew, J.P., Wang, Y., 1992. Accurate and simple analytic representation of the electron-gas correlation energy. Phys. Rev. B Condens. Matter Mater. Phys. 45, 13244–13249.

Pohl, L.R., Schulick, R.D., Highet, R.J., George, J.W., 1984. Reductive-oxygenation mechanism of metabolism of carbon tetrachloride to phosgene by cytochrome P-450. Mol. Pharmacol. 25, 318–321.

Ren, X., Geng, N., Zhang, H., Wang, F., Gong, Y., Song, X., Luo, Y., Zhang, B., Chen, J., 2019. Comparing the disrupting effects of short-, medium- and long-chain chlorinated paraffins on cell viability and metabolism. Sci. Total. Environ. 685, 297–307.

Ren, X., Zhang, H., Geng, N., Xing, L., Zhao, Y., Wang, F., Chen, J., 2018. Developmental and metabolic responses of zebrafish (*Danio rerio*) embryos and larvae to short-chain chlorinated paraffins (SCCPs) exposure. Sci. Total. Environ. 622–623, 214–221.

Rune Toftgård T., H., Eng, L., Halpert, J., 1986. Rat lung and liver microsomal cytochrome p-450 isozymes involved in the hydroxylation of n-hexane. Biochem. Pharm. 35, 3733–3738.

Schoneboom, J.C., Lin, H., Reuter, N., Thiel, W., Cohen, S., Ogliaro, F., Shaik, S., 2002. The elusive oxidant species of cytochrome P450 enzymes: characterization by combined quantum mechanical/molecular mechanical (QM/MM) calculations. J. Am. Chem. Soc. 124, 8142–8151.

Shaik, S., Filatov, M., Schroder, D., Schwarz, H., 1998. Electronic structure makes a difference: cytochrome P-450 mediated hydroxylations of hydrocarbons as a two-state reactivity paradigm. Chem. Eur. J. 4, 193–199.

Shaik, S., Kumar, D., de Visser, S.P., 2008. Valence bond modeling of trends in hydrogen abstraction barriers and transition states of hydroxylation reactions catalyzed by cytochrome P450 enzymes. J. Am. Chem. Soc. 130, 10128–10140.

Shaik, S., Kumar, D., de Visser, S.P., Altun, A., Thiel, W., 2005. Theoretical perspective on the structure and mechanism of cytochrome P450 enzymes. Chem. Rev. 105, 2279–2328.

Shaik, S., Milko, P., Schyman, P., Usharani, D., Chen, H., 2011. Trends in aromatic oxidation reactions catalyzed by cytochrome P450 enzymes: a valence bond modeling. J. Chem. Theory Comput. 7, 327–339.

Staroverov, V.N., Scuseria, G.E., Tao, J., Perdew, J.P., 2003. Comparative assessment of a new nonempirical density functional: molecules and hydrogen-bonded complexes. J. Chem. Phys. 119, 12129–12137.

Strickland, N., Harvey, J.N., 2007. Spin-forbidden ligand binding to the ferrous-heme group: Ab initio and DFT studies. J. Phys. Chem. B 111, 841–852.

Sun, R., Chen, J., Shao, H., Tang, L., Zheng, X., Li, Q.X., Wang, Y., Luo, X., Mai, B., 2020. Bioaccumulation of short-chain chlorinated paraffins in chicken (*Gallus domesticus*): comparison to fish. J. Hazard. Mater. 396, 122590.

Sun, R., Luo, X., Tang, B., Chen, L., Liu, Y., Mai, B., 2017. Bioaccumulation of short chain chlorinated paraffins in a typical freshwater food web contaminated by e-waste in south china: bioaccumulation factors, tissue distribution, and trophic transfer. Environ. Pollut. 222, 165–174.

Tarchouna, Y., Bahri, M., Jaidane, N., Ben Lakhdar, Z., Flament, J.P., 2003. Ab initio transition state theory calculation of the rate constant for the hydrogen abstraction reaction H_2O_2+H → H_2+HO_2. J. Chem. Phys. 118, 1189–1195.

Tripathi, A.C., Upadhyay, S., Paliwal, S., Saraf, S.K., 2018. N1-benzene sulfonyl-2-pyrazolinehybrids in neurological disorders: synthesis, biological screening and computational studies. EXCLI J. 17, 126–148.

Truhlar, D.G., Hase, W.L., Hynes, J.T., 1983. Current status of transition-state theory. J. Phys. Chem. 87, 2664–2682.

UNEP/POPS/COP.8/14., 2017. Recommendation by the Persistent Organic Pollutants Review Committee to list short-chain chlorinated paraffins in Annex A to the Convention and draft text of the proposed amendment.

van Mourik, L.M., Gaus, C., Leonards, P.E.G., de Boer, J., 2016. Chlorinated paraffins in the environment: a review on their production, fate, levels and trends between 2010 and 2015. Chemosphere 155, 415–428.

Wang, F., Zhang, H., Geng, N., Ren, X., Zhang, B., Gong, Y., Chen, J., 2018. A metabolomics strategy to assess the combined toxicity of polycyclic aromatic hydrocarbons (PAHs) and short-chain chlorinated paraffins (SCCPs). Environ. Pollut. 234, 572–580.

Wang, X., Zhu, J., Xue, Z., Jin, X., Jin, Y., Fu, Z., 2019. The environmental distribution and toxicity of short-chain chlorinated paraffins and underlying mechanisms: implications for further toxicological investigation. Sci. Total. Environ. 695, 133834.

Wang, Z., Fu, Z., Yu, Q., Chen, J., 2017. Oxidation reactivity of 1,2-bis(2,4,6-tribromo-phenoxy)ethane (BTBPE) by compound I model of cytochrome P450s. J. Environ. Sci. 62, 11–21.

Warnasuriya, G.D., Elcombe, B.M., Foster, J.R., Elcombe, C.R., 2010. A mechanism for the induction of renal tumours in male Fischer 344 rats by short-chain chlorinated paraffins. Arch. Toxicol. 84, 233–243.

Xia, D., Gao, L., Zheng, M., Li, J., Zhang, L., Wu, Y., Tian, Q., Huang, H., Qiao, L., 2017. Human exposure to short- and medium-chain chlorinated paraffins via mothers' milk in Chinese urban population. Environ. Sci. Technol. 51, 608–615.

Yoshizawa, K., Kagawa, Y., Shiota, Y., 2000. Kinetic isotope effects in a C-H bond dissociation by the iron-oxo species of cytochrome P450. J. Phys. Chem. B 104, 12365–12370.

Yoshizawa, K., Kamachi, T., Shiota, Y., 2001. A theoretical study of the dynamic behavior of alkane hydroxylation by a compound I model of cytochrome P450. J. Am. Chem. Soc. 123, 9806–9816.

Zhang, B., Zhao, B., Xu, C., Zhang, J., 2017. Emission inventory and provincial distribution of short-chain chlorinated paraffins in China. Sci. Total Environ. 581, 582–588.

Zhang, Q., Ji, S.J., Chai, L.H., Yang, F.X., Zhao, M.R., Liu, W.P., Schuurmann, G., Ji, L., 2018. Metabolic Mechanism of aryl phosphorus flame retardants by cytochromes P450: a combined experimental and computational study on triphenyl phosphate. Environ. Sci. Technol. 52, 14411–14421.

Zhang, Q., Wang, J.H., Zhu, J.Q., Liu, J., Zhang, J.Y., Zhao, M.R., 2016. Assessment of the endocrine-disrupting effects of short-chain chlorinated paraffins in in vitro models. Environ. Int. 94, 43–50.

Zhang, W., Gao, Y., Qin, Y., Wang, M., Wu, J., Li, G., An, T., 2019. Photochemical degradation kinetics and mechanism of short-chain chlorinated paraffins in aqueous solution: a case of 1-chlorodecane. Environ. Pollut. 247, 362–370.

Zhao, Y., Truhlar, D.G., 2006. A new local density functional for main-group thermochemistry, transition metal bonding, thermochemical kinetics, and noncovalent interactions. J. Chem. Phys. 125, 194101.

Zhou, J., Chen, J., Liang, C.H., Xie, Q., Wang, Y.N., Zhang, S., Qiao, X., Li, X., 2011. Quantum chemical investigation on the mechanism and kinetics of PBDE photooxidation by ·OH: a case study for BDE-15. Environ. Sci. Technol. 45, 4839–4845.

Zhuo, M.H., Ma, S.T., Li, G.Y., Yu, Y.X., An, T.C., 2019. Chlorinated paraffins in the indoor and outdoor atmospheric particles from the Pearl River Delta: characteristics, sources, and human exposure risks. Sci. Total Environ. 650, 1041–1049.